Sparse Array Beampattern Synthesis via Majorization-Based ADMM

Tong Wei, Linlong Wu, and Bhavani Shankar M. R.
Interdisciplinary Centre for Security, Reliability and Trust (SnT), University of Luxembourg
Email: {tong.wei, linlong.wu, bhavani.shankar}@uni.lu

2021 IEEE 94th Vehicular Technology Conference (VTC2021-Fall) | 978-1-6654-1368-8/21/$31.00 ©2021 IEEE | DOI: 10.1109/VTC2021-FALL52928.2021.9625517

***Abstract*—Beampattern synthesis is a key problem in many wireless applications. With the increasing scale of MIMO antenna array, it is highly desired to conduct beampattern synthesis on a sparse array to reduce the power and hardware cost. In this paper, we consider conducting beampattern synthesis and sparse array construction jointly. In the formulated problem, the beampattern synthesis is designed by minimizing the matching error to the beampattern template, and the Shannon entropy function is first introduced to impose the sparsity of the array. Then, for this nonconvex problem, an iterative method is proposed by leveraging on the alternating direction multiplier method (ADMM) and the majorization minimization (MM). Simulation results demonstrate that, compared with the benchmark, our approach achieves a good trade-off between array sparsity and beampattern matching error with less runtime.**

***Index Terms*—Sparse array, Shannon entropy function, beampattern synthesis, majorization-minimization, ADMM.**

I. Introduction

Beampattern synthesis aims to design the appropriate weight vector to achieve a desired radiation pattern. It has been and continues to be a widely researched topic in radar and wireless communication systems [1]–[3]. Especially for the latter, the beamforming technique expresses several advantages, including improved signal to interference and noise ratio (SINR), reduced interference and enhanced security [4].

Recently, sparse array structures have attracted the significant research interest due to their inherent capability in source localization, simplified feeding networks and the reduced hardware cost and power consumption [5]–[7]. With regards to beampattern synthesis, the sparse array configuration with the minimum number of elements is also required to achieve a specified performance [8], [9]. Specifically, we aim to design a desired beampattern by selecting only a few elements from a predefined array. On the one hand, all the antenna resources need to be exploited to flexibly achieve different beampatterns; on the other hand, the sparse configuration is expected to reduce the overall system cost and power consumption. Hence, beampattern synthesis and antenna selection should be considered simultaneously in order to achieve an appropriate trade-off between these two requirements.

In general, the problem of sparse array beampattern design usually formulated as ℓ_0-norm minimization problem with a predefined pattern shape constraint [8], [10]–[12]. The central problem in these works is the formulation of different methodologies to solve the ℓ_0-norm optimization problem. In [8], the weighted ℓ_1-norm is first utilized to approximate the nonconvex ℓ_0-norm. Then, an iterative method is introduced to solve the second-order cone programming (SOCP) problem. To further improve the sparsity of the solution, the ℓ_p-norm regularization, where $0 < p < 1$, is used in [10], and then the alternating direction multiplier method (ADMM) framework is directly utilized to deal with the nonconvex optimization problem. Recently, the optimal selection vector (or matrix) is introduced in beampattern design when the prior information (i.e. sparsity level) is provided [13]–[15]. However, all the aforementioned methods cannot balance the beampattern design and the sparsity of array configuration simultaneously.

In this paper, we consider the problem of sparse array beampattern synthesis. Compared with the existing weighted ℓ_1-norm algorithms [7], [8], the Shannon entropy regularization, which can simultaneously improve the sparsity level and increase the value of nonzero weight, is first utilized to better prompt the sparsity of array configuration. Meanwhile, different from [13]–[15], the proposed method does not require to predefine the sparsity level. The resulting nonconvex problem is effectively solved by the majorization-based ADMM, which combines the majorization minimization (MM) and the ADMM. Numerical results demonstrate the effectiveness of the proposed method, both in terms of convergence and balance between sparsity and beamshaping.

Notations: $(\cdot)^T$, $(\cdot)^*$ and $(\cdot)^H$ denote transpose, conjugate, and Hermitian transpose, respectively. $\Re(\cdot)$ denotes the real part of a complex value. $\mathbf{1}$ and $\mathbf{I}$ denote all one vector and the identity matrix, respectively. $\|\cdot\|_p$ denotes ℓ_p-norm.

II. Problem Formulation

Let us consider a transmit array with N isotropic antennas uniformly placed with the inter-element spacings d. Then, the corresponding transmit steering vector is

$$\mathbf{a}(\theta) = [1, e^{j\frac{2\pi}{\nu}d\sin(\theta)}, \cdots, e^{j\frac{2\pi}{\nu}(N-1)d\sin(\theta)}]^T \in \mathbb{C}^{N\times 1}, \quad (1)$$

where θ belongs to the whole angle space $\Theta \triangleq [-90^\circ, +90^\circ]$ and ν denotes the wavelength. The transmit beampattern is given by

$$P(\theta) = \mathbf{w}^H \mathbf{A}(\theta)\mathbf{w}, \quad (2)$$

where $\mathbf{A}(\theta) = \mathbf{a}(\theta)\mathbf{a}^H(\theta)$ and $\mathbf{w} = [w_1, w_2, \cdots, w_N]^T \in \mathbb{C}^{N\times 1}$ denotes the weight vector. Without loss of generality, we set $\|\mathbf{w}\|_2^2 = 1$, which means that the array operates in the maximal power model.

In practice, especially for a large-scale array, it is desired to reduce the hardware cost and power consumption, which can be achieved by deploying a sparse array. Mathematically, sparsity regularization will be imposed into the beampattern design formulation, in which the array sparsity and the beampattern should be well balanced. In light of this trade-off, the problem of interested is formulated as

$$\begin{aligned} \min_{\alpha,\mathbf{w}} \quad & \lambda \sum_{k=1}^{K} \|\mathbf{w}^H \mathbf{A}(\theta_k)\mathbf{w} - \alpha d(\theta_k)\|_2^2 + f(\mathbf{w}) \\ s.t. \quad & \|\mathbf{w}\|_2^2 = 1, \end{aligned} \tag{3}$$

where λ is the trade-off parameter, $f(\mathbf{w})$ denotes the sparsity-promoting regularization function, θ_k denotes the k-th angle within the angle space Θ and α is used to scale the desired beampattern $d(\theta_k)$.

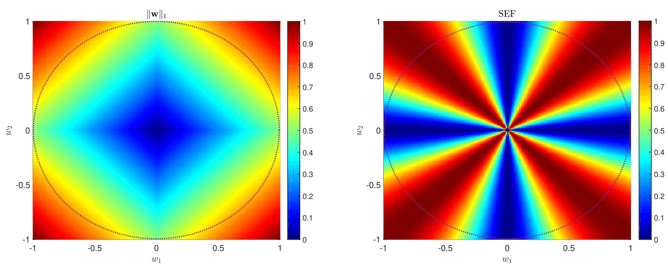

Fig. 1. Comparison of different sparsity-promoting regularization functions.

It is noted that there exist various choices to promote the sparse solution of problem (3). For example, the well-known ℓ_1-norm is utilized to achieve the sparsity solution [7], [8]. Recently, the Shannon entropy function (SEF) is being widely used in compressed sensing [16], [17], due to its ability to measure the concentration and diversity of a vector. Its definition in terms of $\mathbf{w}$ is given by

$$f(\mathbf{w}) = \sum_{n=1}^{N} \left(\frac{|w_n|^2}{\|\mathbf{w}\|_2^2} \right) \log \frac{|w_n|^2}{\|\mathbf{w}\|_2^2}. \tag{4}$$

Fig.1 compares the commonly used ℓ_l-norm with the SEF. It is seen that both of them can prompt sparsity. However, the SEF can simultaneously improve the sparsity level and increase the value of nonzero entries of $\mathbf{w}$. Especially on unit sphere, i.e., $\|\mathbf{w}\|_2^2 = 1$, the SEF has better sparsity-promoting ability compared with ℓ_1-norm. Due to the superior properties of the SEF, in this paper, we consider it as the sparsity-promoting regularizer in problem (3).

III. Majorization-Based ADMM Optimization Algorithm

Note that problem (3) is still nonconvex due to both the objective function and the constraint. Hence, we will derive an iterative algorithm based on the powerful MM and ADMM frameworks. To tackle the nonconvex quartic objective, we introduce an auxiliary variable $\mathbf{v} \in \mathbb{C}^{N\times 1}$ to convert problem (3) into

$$\begin{aligned} \min_{\alpha,\mathbf{w},\mathbf{v}} \quad & \lambda\varphi(\alpha,\mathbf{v},\mathbf{w}) + f(\mathbf{w}) \\ s.t. \quad & \mathbf{w} - \mathbf{v} = \mathbf{0} \\ & \|\mathbf{w}\|_2^2 = 1, \end{aligned} \tag{5}$$

where $\varphi(\alpha,\mathbf{v},\mathbf{w}) = \sum_{k=1}^{K} \|\mathbf{w}^H\mathbf{A}(\theta_k)\mathbf{v} - \alpha d(\theta_k)\|_2^2$. Then, the augmented Lagrangian of problem (5) is

$$\begin{aligned} \mathcal{L}(\alpha,\mathbf{v},\mathbf{w},\mathbf{u}) &= \lambda \sum_{k=1}^{K} \|\mathbf{w}^H\mathbf{A}(\theta_k)\mathbf{v} - \alpha d(\theta_k)\|_2^2 + f(\mathbf{w}) \\ &\quad + \boldsymbol{\gamma}^H(\mathbf{w}-\mathbf{v}) + \frac{\rho}{2}\|\mathbf{w}-\mathbf{v}\|_2^2 \\ &= \lambda \sum_{k=1}^{K} \|\mathbf{w}^H\mathbf{A}(\theta_k)\mathbf{v} - \alpha d(\theta_k)\|_2^2 + f(\mathbf{w}) \\ &\quad + \frac{\rho}{2}\|\mathbf{w}-\mathbf{v}+\mathbf{u}\|_2^2 + const. \end{aligned} \tag{6}$$

where $\mathbf{u} = \frac{1}{\rho}\boldsymbol{\gamma}$ denotes the dual variable [18] and ρ is a positive penalty parameter. Within the framework of ADMM, the update rules at the $(t+1)$-th iteration are given by

$$\alpha^{(t+1)} := \operatorname*{argmin}_{\alpha} \ \mathcal{L}(\alpha,\mathbf{v}^{(t)},\mathbf{w}^{(t)},\mathbf{u}^{(t)}), \tag{7a}$$

$$\mathbf{v}^{(t+1)} := \operatorname*{argmin}_{\mathbf{v}} \ \mathcal{L}(\alpha^{(t+1)},\mathbf{v},\mathbf{w}^{(t)},\mathbf{u}^{(t)}), \tag{7b}$$

$$\mathbf{w}^{(t+1)} := \operatorname*{argmin}_{\|\mathbf{w}\|_2^2=1} \ \mathcal{L}(\alpha^{(t+1)},\mathbf{v}^{(t+1)},\mathbf{w},\mathbf{u}^{(t)}), \tag{7c}$$

$$\mathbf{u}^{(t+1)} := \mathbf{u}^{(t)} + (\mathbf{w}^{(t+1)} - \mathbf{v}^{(t+1)}). \tag{7d}$$

A. Update of α

At the $(t+1)$-th iteration, given $\mathbf{v}^{(t)}$ and $\mathbf{w}^{(t)}$, the optimization problem (7a) can be written as

$$\min_{\alpha} \quad \sum_{k=1}^{K} \|\mathbf{w}^{(t)H}\mathbf{A}(\theta_k)\mathbf{v}^{(t)} - \alpha d(\theta_k)\|_2^2, \tag{8}$$

which has the closed-form solution

$$\alpha^{(t+1)} = \frac{\Xi_1^{(t)}}{\sum_{k=1}^{K} d^2(\theta_k)}, \tag{9}$$

with $\Xi_1^{(t)} = \sum_{k=1}^{K} 2d(\theta_k)\Re\left(\mathbf{w}^{(t)H}\mathbf{A}(\theta_k)\mathbf{v}^{(t)}\right)$.

B. Update of $\mathbf{v}$

At the $(t+1)$-th iteration, given $\alpha^{(t+1)}$, $\mathbf{w}^{(t)}$ and $\mathbf{u}^{(t)}$, we can update $\mathbf{v}$ by solving the following problem

$$\min_{\mathbf{v}} \quad \lambda\varphi(\alpha^{(t+1)},\mathbf{v},\mathbf{w}^{(t)}) + \frac{\rho}{2}\|\mathbf{w}^{(t)} - \mathbf{v} + \mathbf{u}^{(t)}\|_2^2. \tag{10}$$

Noticed that problem (10) is an unconstrained quadratic programming problem and hence convex. By setting the derivative of objective function of (10) with respect to $\mathbf{v}^*$ to be zero, we have

$$\Xi_2^{(t)}\mathbf{v} - \boldsymbol{\Upsilon}_2^{(t+1)}\mathbf{w}^{(t)} + \frac{\rho}{2}\left(\mathbf{v} - (\mathbf{w}^{(t)} + \mathbf{u}^{(t)})\right) = \mathbf{0} \tag{11}$$

where

$$\mathbf{\Xi}_2^{(t)} = \lambda \sum_{k=1}^{K} \mathbf{A}^H(\theta_k)\mathbf{w}^{(t)}{\mathbf{w}^{(t)}}^H \mathbf{A}(\theta_k), \tag{12a}$$

$$\mathbf{\Upsilon}_2^{(t+1)} = \lambda \sum_{k=1}^{K} \alpha^{(t+1)} d(\theta_k)\mathbf{A}^H(\theta_k). \tag{12b}$$

The solution to (11) is

$$\mathbf{v}^{(t+1)} = (\mathbf{\Xi}_2^{(t)} + \frac{\rho}{2}\mathbf{I})^{-1}(\mathbf{\Upsilon}_2^{(t+1)}\mathbf{w}^{(t)} + \frac{\rho}{2}(\mathbf{w}^{(t)} + \mathbf{u}^{(t)})), \tag{13}$$

which is also the optimal solution to problem (10).

C. Update of $\mathbf{w}$

At the $(t+1)$-th iteration, given $\alpha^{(t+1)}$, $\mathbf{v}^{(t+1)}$, $\mathbf{w}^{(t)}$ and $\mathbf{u}^{(t)}$, we can update $\mathbf{w}$ into solving the following problem

$$\begin{aligned} \min_{\mathbf{w}} \quad & \lambda\varphi(\alpha^{(t+1)}, \mathbf{v}^{(t+1)}, \mathbf{w}) + f(\mathbf{w}) \\ & + \frac{\rho}{2}\|\mathbf{w} - \mathbf{v}^{(t+1)} + \mathbf{u}^{(t)}\|_2^2 \\ s.t. \quad & \|\mathbf{w}\|_2^2 = 1. \end{aligned} \tag{14}$$

Due to the concave nature of $f(\mathbf{w})$, it is difficult to directly solve problem (14). Thus, we resort to the majorization-minimization (MM) framework [19], [20], and solving the problem (14) is then transformed to solving a series of subproblems until convergence.

To begin with, let us introduce an important majorizing function of $f(\mathbf{w})$ via the following Lemma.

Lemma 1. *For any complex set* $\mathbf{w} \in \mathbb{C}^{N\times 1}$ *with* $\|\mathbf{w}\|_2^2 = 1$*, we always have*

$$f(\mathbf{w}) = g(\widetilde{\mathbf{w}}) \leq \mathbf{w}^H \mathbf{D}_t \mathbf{w} + const. \tag{15}$$

where $\widetilde{\mathbf{w}} = \mathbf{w} \odot \mathbf{w}^*$, $g(\widetilde{\mathbf{w}}) = -\sum_{n=1}^{N} \widetilde{w}_n \log \widetilde{w}_n$, $const. = g(\widetilde{\mathbf{w}}^{(t)}) - \nabla g(\widetilde{\mathbf{w}}^{(t)})^T \widetilde{\mathbf{w}}^{(t)}$, $\mathbf{D}_t = \mathrm{diag}(\nabla g(\widetilde{\mathbf{w}}^{(t)}))$ *and* $\nabla g(\widetilde{\mathbf{w}}^{(t)})$ *is the gradient vector with the* n*-th element* $\nabla g(\widetilde{w}_n^{(t)}) = -\log \widetilde{w}_n^{(t)} - 1, n = 1, \cdots, N$.

Proof: Recalling the constraint $\|\mathbf{w}\|_2^2 = 1$, we have

$$f(\mathbf{w}) = -\sum_{n=1}^{N} w_n w_n^* \log w_n w_n^*. \tag{16}$$

Hence, it is easily derived that $f(\mathbf{w}) = g(\widetilde{\mathbf{w}})$. Then, the upper bound function of $g(\widetilde{\mathbf{w}})$ at current point $\widetilde{\mathbf{w}}^{(t)}$ is

$$\begin{aligned} g(\widetilde{\mathbf{w}}) &\leq g(\widetilde{\mathbf{w}}^{(t)}) + \nabla g(\widetilde{\mathbf{w}}^{(t)})^T(\widetilde{\mathbf{w}} - \widetilde{\mathbf{w}}^{(t)}) \\ &= \nabla g(\widetilde{\mathbf{w}}^{(t)})^T(\mathbf{w} \odot \mathbf{w}^*) + const. \\ &= \mathbf{w}^H \mathbf{D}_t \mathbf{w} + const. \end{aligned} \tag{17}$$

where $const. = g(\widetilde{\mathbf{w}}^{(t)}) - \nabla g(\widetilde{\mathbf{w}}^{(t)})^T \widetilde{\mathbf{w}}^{(t)}$ and $\nabla g(\widetilde{\mathbf{w}}^{(t)})$ stands for the derivative of $g(\widetilde{\mathbf{w}}^{(t)})$ with respect $\widetilde{\mathbf{w}}^{(t)}$, whose n-th entry is

$$\nabla g(\widetilde{w}_n^{(t)}) = -\log \widetilde{w}_n^{(t)} - 1, n = 1, \cdots, N. \tag{18}$$

Based on above, we conclude that (15) is satisfied, thereby completing the proof. ■

Algorithm 1 Majorization-based ADMM for Problem (3)

Input: $N, \lambda, \rho, \eta, \mathbf{A}(\theta_k), d(\theta_k), k = 1, \cdots, K$
Initalize: $\alpha^{(0)}, \mathbf{v}^{(0)}, \mathbf{w}^{(0)}$, $\mathbf{u}^{(0)}$ and counter $t = 0$
repeat
  Update $\alpha^{(t+1)}$ using (9)
  Update $\mathbf{v}^{(t+1)}$ using (13)
  Calculate gradient vector $\nabla g(\widetilde{\mathbf{w}}^{(t)})$ via (18)
  Reconstruct the diagonal matrix $\mathbf{D}_t$ using $\nabla g(\widetilde{\mathbf{w}}^{(t)})$
  Update $\mathbf{w}^{(t+1)}$ using (23)
  Update $\mathbf{u}^{(t+1)}$ using (24)
  Counter Increase: $t \leftarrow t+1$
until $\|\mathbf{w}^{(t+1)} - \mathbf{w}^{(t)}\|_2 \leq \eta$
Output: $\mathbf{w}^\star = \mathbf{w}^{(t)}$

Hence, replacing the function $f(\mathbf{w})$ by its majorizer from (15) and ignoring the constants, problem (14) can be simplified as follows

$$\begin{aligned} \min_{\mathbf{w}} \quad & \lambda\varphi(\alpha^{(t+1)}, \mathbf{v}^{(t+1)}, \mathbf{w}) + \mathbf{w}^H \mathbf{D}_t \mathbf{w} \\ & + \frac{\rho}{2}\|\mathbf{w} - \mathbf{v}^{(t+1)} + \mathbf{u}^{(t)}\|_2^2 \\ s.t. \quad & \|\mathbf{w}\|_2^2 = 1. \end{aligned} \tag{19}$$

Noted that problem (19) is difficult to obtain the global optimal solution due to the nonconvex unit sphere constraint. Even though this kind of problem can be solved by semidefinite relaxation (SDR) [21], the corresponding problem size will greatly grow which leads to higher computational complexity. Herein, we utilize a more effective method, which named projected gradient descent (PGD) [22], to tackle problem (19). Specifically, we can first remove the unit sphere constraint and solve the unconstrained problem. Then, the projection operator is utilized to project the solution onto unit sphere.

Setting the derivative of objective function of (19) with respect to $\mathbf{w}^*$ as zero, we have

$$\mathbf{\Xi}_3^{(t+1)}\mathbf{w} - \mathbf{\Upsilon}_3^{(t+1)}\mathbf{v}^{(t+1)} + \mathbf{D}_t\mathbf{w} + \frac{\rho}{2}(\mathbf{w} - (\mathbf{v}^{(t+1)} - \mathbf{u}^{(t)})) = \mathbf{0} \tag{20}$$

where

$$\mathbf{\Xi}_3^{(t+1)} = \lambda \sum_{k=1}^{K} \mathbf{A}(\theta_k)\mathbf{v}^{(t+1)}{\mathbf{v}^{(t+1)}}^H \mathbf{A}^H(\theta_k), \tag{21a}$$

$$\mathbf{\Upsilon}_3^{(t+1)} = \lambda \sum_{k=1}^{K} \alpha^{(t+1)} d(\theta_k)\mathbf{A}(\theta_k). \tag{21b}$$

According to (20), it is concluded that

$$\widehat{\mathbf{w}}^{(t+1)} = (\mathbf{\Xi}_3^{(t+1)} + \mathbf{D}_t + \frac{\rho}{2}\mathbf{I})^{-1}(\mathbf{\Upsilon}_3^{(t+1)}\mathbf{v}^{(t+1)} + \frac{\rho}{2}(\mathbf{v}^{(t+1)} - \mathbf{u}^{(t)})). \tag{22}$$

The solution to (19) is

$$\mathbf{w}^{(t+1)} = \mathcal{P}(\widehat{\mathbf{w}}^{(t+1)}) \tag{23}$$

where $\mathcal{P}(\cdot) = (\cdot)/\|\cdot\|_2$ denotes the spherical projection.

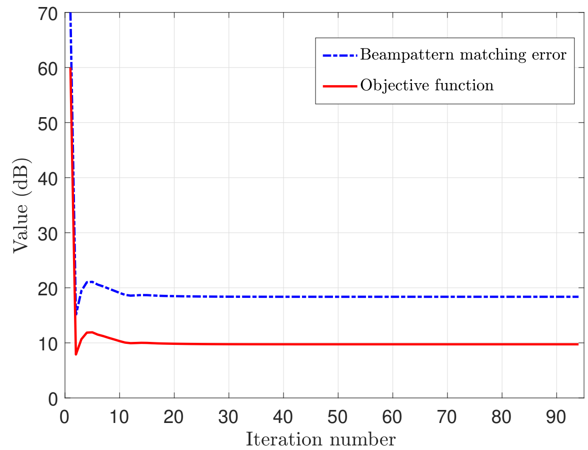

Fig. 2. Convergence of the objective and beampattern matching; selected number of elements, $\hat{N} = 18$.

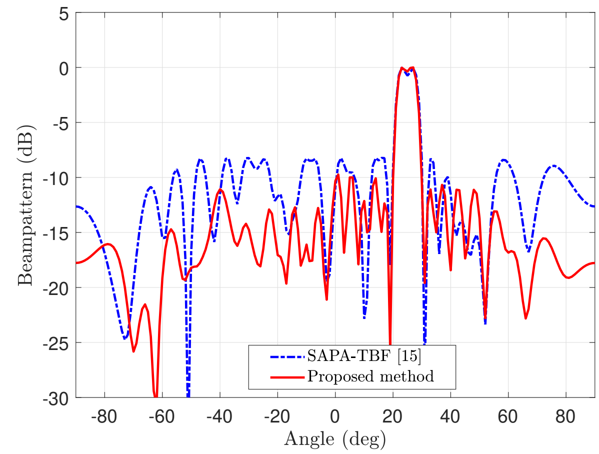

Fig. 3. Beampattern comparison, $\hat{N} = 18$.

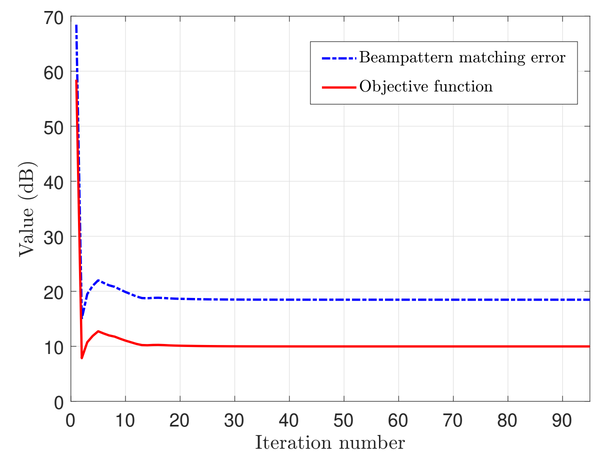

Fig. 4. Convergence of the objective and beampattern matching; selected number of elements, $\hat{N} = 20$.

D. Update of $\mathbf{u}$

At the $(t+1)$-th iteration, given $\mathbf{v}^{(t+1)}$, $\mathbf{w}^{(t+1)}$ and $\mathbf{u}^{(t)}$, the dual variable can be directly updated as

$$\mathbf{u}^{(t+1)} = \mathbf{u}^{(t)} + (\mathbf{w}^{(t+1)} - \mathbf{v}^{(t+1)}). \tag{24}$$

According to above discussions, the proposed majorization-based ADMM based algorithm for solving problem (3) is summarized in **Algorithm 1**.

IV. Simulation Results

In this section, some representative numerical examples are provided to evaluate the performance of proposed method for sparse array transmit beampattern synthesis. Herein, the spatial domain $\Theta \triangleq [-90°, +90°]$ is uniformly sampled with step-size $1°$. Further, the initial value of $\mathbf{v}^{(0)}$ and $\mathbf{w}^{(0)}$ are randomly generated from zero-mean complex Gaussian distribution and normalized to $\|\mathbf{v}^{(0)}\|_2^2 = 1$ and $\|\mathbf{w}^{(0)}\|_2^2 = 1$. Meanwhile, we set $\alpha^{(0)} = 1$ and $\mathbf{u}^{(0)} = \mathbf{0}$. Throughout the simulations, other parameters are set as $N = 30$, $\lambda = 0.1$, $\rho = 30$ and $\eta = 10^{-8}$. Finally $\hat{N}$ denotes the number of selected antennas.

A. Beampattern with a single mainlobe

In this example, we consider a mainlobe spanning $\Theta_m = [22°, 28°]$ and let the desired pattern as $d(\theta_m) = 1000, \theta_m \in \Theta_m$. Fig.2 demonstrates the convergence performance of proposed method. It is seen that the proposed method expresses good convergence performance for both objective value and beampattern matching within 100 iterations. Fig.3 compares the synthesized beampatterns. The benchmark method, named SAPA-TBF [15], needs to predefine the sparsity level first and then minimize the maximal difference between the designed beamapttern and the desired one. For comparison, we set $\hat{N} = 18$ for SAPA-TBF, which is the number of selected elements of our proposed method. It is seen from Fig.3 that the proposed method has relatively lower sidelobes than SAPA-TBF. And the normalized beampattern matching error of proposed method is -1.651 dB compared with 2.628 dB for SAPA-TBF method. Meanwhile, in [15], it is proved that SAPA-TBF has better beampattern synthesis performance than the ℓ_p-norm based method [10].

B. Beampattern with two mainlobes

In this example, we consider the two mainlobes which are located in $\Theta_m = [-15°, -11°] \cup [11°, 15°]$. Meanwhile, the desired beampattern is set as $d(\theta_m) = 1000, \theta_m \in \Theta_m$. We set $\hat{N} = 20$ for SAPA-TBF. Fig.4 expresses the convergence performance of proposed method. Again, the proposed method still has good convergence performance within 100 iterations. Fig.5 compares the synthesized beampatterns. It is observed that our method has a lower peak side level than SAPA-TBF. The corresponding normalized beampattern matching error for our method is 0.869 dB, while 3.838 dB in [15], indicating improved performance of our method in beampattern matching.

Table 1. compares the cardinality, required runtime and normalized beampattern matching error of these two methods.

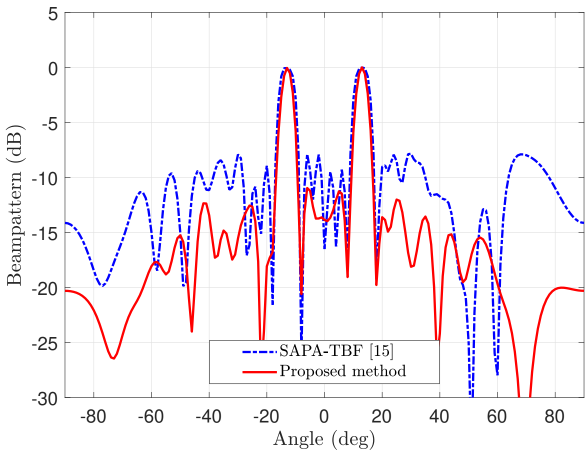

Fig. 5. Beampattern comparison , $\hat{N} = 20$.

TABLE I
THE PERFORMANCE COMPARISON OF DIFFERENT METHODS.

Method	Single mainlobe		Two mainlobes	
	Proposed	SAPA-TBF	Proposed	SAPA-TBF
Cardinality	18	18	20	20
Runtime (s)	2.75	46.272	2.97	52.955
Matching error (dB)	-1.651	2.628	0.869	3.838

It is seen that, with the same selected antennas, the proposed method has the smaller beampattern matching error compared with SAPA-TBF. Meanwhile, our method is more efficiency than SAPA-TBF in terms of runtime.

V. Conclusion

In this paper, a new sparse array beampattern design method is proposed. To prompt the sparsity of array configuration, the Shannon entropy function is imposed. However, the resulting optimization problem, which has the summation of quadratic and concave objective function, is highly nonconvex. Hence, the majorization-based ADMM algorithm is developed to solve this problem. Compared to the existing method, the proposed algorithm shows improvements in terms of beampattern matching and computational efficiency, rendering it attractive for use in radar and wireless communication systems.

Acknowledgment

This work was supported by the Luxembourg National Research Fund (FNR) through the CORE project "SPRINGER" under Grant R-STR-5010-00-B/SPRINGER.

References

[1] H. He, P. Stoica, and J. Li, "Wideband MIMO systems: Signal design for transmit beampattern synthesis," *IEEE Transactions on Signal Processing*, vol. 59, no. 2, pp. 618–628, 2011.

[2] B. Chen, X. Chen, Y. Huang, and J. Guan, "Transmit beampattern synthesis for the FDA radar," *IEEE Antennas and Wireless Propagation Letters*, vol. 17, no. 1, pp. 98–101, 2018.

[3] W.-Q. Wang and Z. Zheng, "Hybrid MIMO and phased-array directional modulation for physical layer security in mmwave wireless communications," *IEEE Journal on Selected Areas in Communications*, vol. 36, no. 7, pp. 1383–1396, 2018.

[4] Y. Alsaba, S. K. A. Rahim, and C. Y. Leow, "Beamforming in wireless energy harvesting communications systems: A survey," *IEEE Communications Surveys Tutorials*, vol. 20, no. 2, pp. 1329–1360, 2018.

[5] P. Pal and P. P. Vaidyanathan, "Nested arrays: A novel approach to array processing with enhanced degrees of freedom," *IEEE Transactions on Signal Processing*, vol. 58, no. 8, pp. 4167–4181, 2010.

[6] E. BouDaher, Y. Jia, F. Ahmad, and M. G. Amin, "Multi-frequency co-prime arrays for high-resolution direction-of-arrival estimation," *IEEE Transactions on Signal Processing*, vol. 63, no. 14, pp. 3797–3808, 2015.

[7] B. Fuchs, "Synthesis of sparse arrays with focused or shaped beampattern via sequential convex optimizations," *IEEE Transactions on Antennas and Propagation*, vol. 60, no. 7, pp. 3499–3503, 2012.

[8] S. E. Nai, W. Ser, Z. L. Yu, and H. Chen, "Beampattern synthesis for linear and planar arrays with antenna selection by convex optimization," *IEEE Transactions on Antennas and Propagation*, vol. 58, no. 12, pp. 3923–3930, 2010.

[9] S. A. Hamza and M. G. Amin, "Sparse array design for transmit beamforming," in *2020 IEEE International Radar Conference (RADAR)*, 2020, pp. 560–565.

[10] J. Liang, X. Zhang, H. C. So, and D. Zhou, "Sparse array beampattern synthesis via alternating direction method of multipliers," *IEEE Transactions on Antennas and Propagation*, vol. 66, no. 5, pp. 2333–2345, 2018.

[11] R. C. Nongpiur and D. J. Shpak, "Synthesis of linear and planar arrays with minimum element selection," *IEEE Transactions on Signal Processing*, vol. 62, no. 20, pp. 5398–5410, 2014.

[12] T. Hong, X. Shi, and X. Liang, "Synthesis of sparse linear array for directional modulation via convex optimization," *IEEE Transactions on Antennas and Propagation*, vol. 66, no. 8, pp. 3959–3972, 2018.

[13] B. Fuchs, "Antenna selection for array synthesis problems," *IEEE Antennas and Wireless Propagation Letters*, vol. 16, pp. 868–871, 2017.

[14] Z. Zheng, Y. Fu, and W. Q. Wang, "Sparse array beamforming design for coherently distributed sources," *IEEE Transactions on Antennas and Propagation*, pp. 1–1, 2020.

[15] W. Fan, J. Liang, X. Fan, and H. C. So, "A unified sparse array design framework for beampattern synthesis," *Signal Processing*, vol. 182, p. 107930, 2021.

[16] S. Huang and T. D. Tran, "Sparse signal recovery via generalized entropy functions minimization," *IEEE Transactions on Signal Processing*, vol. 67, no. 5, pp. 1322–1337, 2019.

[17] P. Xiao, B. Liao, and J. Li, "One-bit compressive sensing via Schur-concave function minimization," *IEEE Transactions on Signal Processing*, vol. 67, no. 16, pp. 4139–4151, 2019.

[18] P. Xiao, P. Chu, and B. Liao, "ADMM-based approach for compressive sensing with negative weights," *IET Signal Processing*, vol. 14, pp. 854–860(6), 2020. [Online]. Available: https://digital-library.theiet.org/content/journals/10.1049/iet-spr.2020.0276

[19] C. Lu, J. Feng, S. Yan, and Z. Lin, "A unified alternating direction method of multipliers by majorization minimization," *IEEE Transactions on Pattern Analysis and Machine Intelligence*, vol. 40, no. 3, pp. 527–541, 2018.

[20] Y. Sun, P. Babu, and D. P. Palomar, "Majorization-minimization algorithms in signal processing, communications, and machine learning," *IEEE Transactions on Signal Processing*, vol. 65, no. 3, pp. 794–816, 2017.

[21] Z.-Q. Luo, N. D. Sidiropoulos, P. Tseng, and S. Zhang, "Approximation bounds for quadratic optimization with homogeneous quadratic constraints," *SIAM Journal on Optimization*, vol. 18, no. 1, pp. 1–28, 2007. [Online]. Available: https://doi.org/10.1137/050642691

[22] T. Vu, R. Raich, and X. Fu, "On convergence of projected gradient descent for minimizing a large-scale quadratic over the unit sphere," in *2019 IEEE 29th International Workshop on Machine Learning for Signal Processing (MLSP)*, 2019, pp. 1–6.